VOL. 10, NO. 8, MAY 2015 ISSN 1819-6608
ARPN Journal of Engineering and Applied Sciences


www.arpnjournals.com

PRESSURE BEHAVIOR OF HORIZONTAL WELLS IN DUAL-POROSITY, DUAL-PERMEABILITY NATURALLY-FRACTURED RESERVOIRS

Jing Lu[1], Tao Zhu[1], Djebbar Tiab[2] and Freddy Humberto Escobar[3]
[1]Department of Petroleum Engineering, the Petroleum Institute, Abu Dhabi, U.A.E.
[2]The University of Oklahoma, 100 Boyd., Norman, OK, EE.UU.
[3]Universidad Surcolombiana/CENIGAA, Avenida Pastrana - Cra 1, Neiva, Huila, Colombia
E-Mail: fescobar@usco.edu.co

ABSTRACT

The pressure behavior of horizontal wells in dual-porosity, dual-permeability naturally-fractured reservoirs is presented. The proposed equation is obtained by double Fourier transformation and Laplace transformation. The results calculated for combinations of various dimensionless characterizing parameters, including the permeability ratio between matrix and fracture systems, have revealed the unique behavior of naturally fractured reservoirs when the flow state within the matrix blocks is taken into account. It is concluded that, for the flow within matrix blocks will weaken the essential nature of fluid flow through a dual-porosity, single permeability medium revealed by Warren-Root model. This paper also presents the application of "Tiab's Direct Synthesis" technique to horizontal wells in an infinite-acting dual-porosity, dual-permeability naturally-fractured reservoirs with pseudosteady state interporosity flow.

Keywords: pressure transient analysis, *TDS* technique, naturally fractured reservoirs, dual permeability systems.

1. INTRODUCTION

The pressure behavior of naturally fractured reservoirs (NFRs) is usually studied using Warren and Root (1963) simplified model neglecting the flow of fluids in the matrix blocks. This simplification generally yields satisfactory results because the matrix permeability is usually much less than that of the fracture system in a naturally fractured reservoir. However, in order to determine the limits of validity of Warren and Root's solution and to study the behavior of a naturally fractured reservoir in which the contrast between the permeability of matrix system and that of fracture system is not significant, the more general Barenblatt-Zheltov-Kochina (1960) model is typically used in the literature. But the analytical solutions to this model which were obtained by numerical analysis or numerical inversion are very complex and inconvenient to use (Chen and Jiang, 1980).

Horizontal wells have been proven to be an effective means of producing hydrocarbons from naturally fractured reservoirs. Extension of horizontal well solutions to naturally fractured reservoirs was originally developed by Rosa and Carvalho (1988) using instantaneous source functions. They developed a relationship to determine the naturally fractured, dual-porosity solution in terms of the pressure derivatives in Laplace space. Aguilera and Ng (1991) applied the transform method developed by Goode and Thambynayagam to drawdown and buildup tests in naturally fractured reservoirs. Their solutions led to the identification of six flow periods, some of which may be dominated by natural fractures.

To the best of our knowledge, all pressure drawdown and buildup equations for horizontal wells in NFRs are based on Warren and Root model, which is a dual-porosity, single permeability model (see Figure-1). This study presents an analytical solution for horizontal wells pressure transient equation in dual-porosity, dual-permeability NFRs. The proposed equation is obtained by double Fourier transformation and Laplace transformation. The results calculated for combinations of various dimensionless characterizing parameters, including the permeability ratio between matrix and fracture systems, have revealed the unique behavior of naturally fractured reservoirs when the flow state within the matrix blocks is taken into account.

Early techniques for interpreting horizontal wells pressure transient tests in NFRs include conventional semi-log and log-log type curve methods. Both methods are accurate provided certain criteria are established. That is, all flow regimes must be observed in the pressure and pressure derivative curve over a sufficient period of time. In NFRs, all flow regimes are rarely observed from pressure data, thus type curve method will have a non-uniqueness problem and semilog analysis will be incomplete. Compound this problem with masking effect of wellbore storage and analysis becomes suspect.

Therefore, it is proposed to use an alternative method referred to as "Tiab's Direct Synthesis" (*TDS*). This method utilizes the characteristic intersection points, slopes, and times of various straight lines from a log-log plot of pressure and pressure derivative data. Values of these points are linked directly to the exact, analytical solutions to obtain reservoir and well parameters.

The *TDS* method has been successfully applied to uniform flux and infinite conductivity vertical fracture models (Tiab, 1989), to vertically fractured wells in closed systems (Tiab, 1994), to homogeneous reservoirs with skin and wellbore storage (Tiab, 1995), to vertical wells and horizontal wells in naturally fractured reservoirs (Engler and Tiab, 1996), and to horizontal wells in anisotropic media (Engler and Tiab, 1996).

This study also presents the application of *TDS* to horizontal wells in an infinite acting dual-porosity, dual-permeability NFR with pseudosteady state interporosity flow. New analytical and empirical expressions are

developed as a result of this study. Natural fracture parameters can be determined from the minimum coordinates of the pressure derivative curve.

2. MATHEMATICAL FORMULATION

Figure-2 is a schematic of a horizontal well. A horizontal well of length L is parallel to x direction. The following assumptions are made:

1) The dual-porosity, dual-permeability naturally fractured reservoir is horizontal, and has constant matrix and fracture permeabilities, thickness, and porosity. Both the matrix system and the fracture system are homogeneous and isotropic.
2) The reservoir has infinite lateral extension, i.e., the boundaries of the reservoir in the horizontal directions are so far away that the pressure disturbance does not travel far enough to reach the boundaries during the well production.
3) The reservoir pressure is initially constant; the initial pressure is uniform throughout the reservoir. The pressure remains constant and equal to the initial value at an infinite distance from the well. The reservoir is bounded by top and bottom impermeable formations.
4) The production occurs through a horizontal well of radius R_w, represented in the model by a uniform line sink located at a distance Z_w from the lower boundary, and the length of the well is L. And the thickness of the formation is small compared to the length of the horizontal well.
5) A single-phase fluid, of small and constant compressibility, C, constant viscosity, μ, and formation volume factor, B, flows from the reservoir to the well. Fluid properties are independent of pressure. Constant flow rate is applied.
6) Pseudo-steady state interporosity flow occurs between the matrix blocks and fractures, both the fracture system and matrix blocks can feed the horizontal wellbore (see Figure-3).
7) Wellbore storage and gravity effects are ignored.

Equations for initial and boundary conditions

As Figure-2 shows, the horizontal well is a uniform line sink in three dimensional space, the coordinates of the two ends are (0, 0, Z_w) and (L, 0, Z_w).

The drainage domain is:

$$\Omega = (-\infty,\infty)\times(-\infty,\infty)\times(0,H) \quad (1)$$

The reservoir has infinite lateral extension i.e., the reservoir has the following outer boundary condition:

$$P_j(r,t) = P_{ini};\ when\ r\to\infty;(j=1,2) \quad (2)$$

Where P_{ini} is the initial pressure throughout the reservoir, subscripts 1 and 2 denote the matrix block system and the fracture system, respectively.

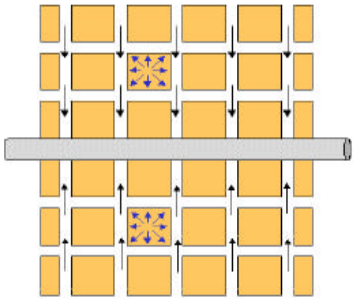

Figure-1. Horizontal well in dual-porosity, single permeability reservoir.

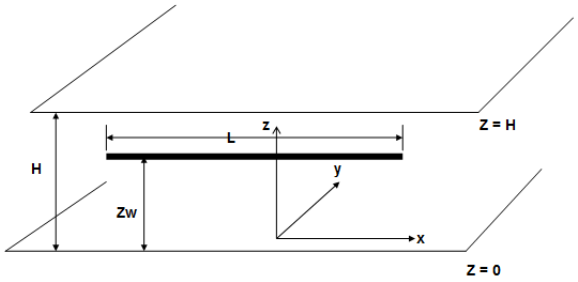

Figure-2. Horizontal well configuration.

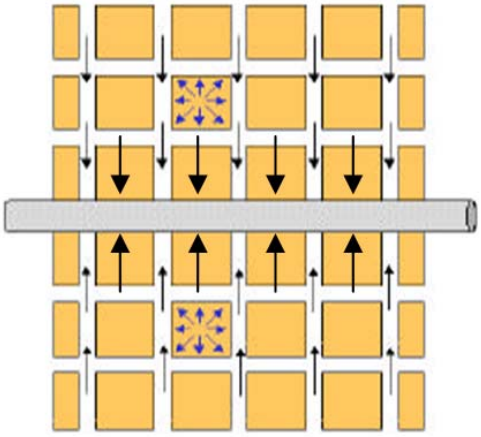

Figure-3. Horizontal well in dual-porosity, dual-permeability reservoir.

Upper and lower reservoir boundaries are impermeable,

$$\frac{\partial P_j}{\partial z}\Big|_{z=0} = \frac{\partial P_j}{\partial z}\Big|_{z=H} = 0;\quad (j=1,2) \quad (3)$$

At wellbore, there holds,

$$P_1(R_w,t) = P_2(R_w,t) = P_w(t) \quad (4)$$

Initial condition:

$$P_j(r,t) = P_{ini};\ when\ t = 0; (j = 1,2) \quad (5)$$

Using continuum mechanics, the medium and flow parameters of the two media, fractures and matrix, are defined at each mathematical point. The pressure equations for a single point sink are derived, then, using Principle of Superposition, the solutions for uniform line sink can be obtained.

Point sink solution

The system of equations for a point sink at (x', 0, Z_w) in the dual-porosity, dual-permeability naturally fractured reservoir is,

$$\frac{\partial^2 P_1}{\partial x^2} + \frac{\partial^2 P_1}{\partial y^2} + \frac{\partial^2 P_1}{\partial z^2} + \alpha(P_2 - P_1) = (\frac{\mu\phi_1 C_1}{K_1})\frac{\partial P_1}{\partial t} + (\frac{\mu B Q_1}{K_1})\delta(x-x')\delta(y)\delta(z-z_w) \quad (6a)$$

$$\frac{\partial^2 P_2}{\partial x^2} + \frac{\partial^2 P_2}{\partial y^2} + \frac{\partial^2 P_2}{\partial z^2} + (\frac{K_1\alpha}{K_2})(P_1 - P_2) = (\frac{\mu\phi_2 C_2}{K_2})\frac{\partial P_2}{\partial t} + (\frac{\mu B Q_2}{K_2})\delta(x-x')\delta(y)\delta(z-z_w) \quad (6b)$$

Define the ratio of matrix system permeability to fracture system permeability below:

$$D = K_1 / K_2 \quad (7a)$$

$$\beta = D/(1+D) \quad (7b)$$

And,

Assume Q_w is the total flow rate of the horizontal well, Q_1 is the flow rate of matrix block system, Q_2 is the flow rate of fracture system, then,

$$Q_w = Q_1 + Q_2 \quad (8)$$

Define

$$\tau_1 = Q_1 / Q_w, \quad \tau_2 = Q_2 / Q_w \quad (9)$$

And assume

$$\tau_1 = K_1/(K_1+K_2), \quad \tau_2 = K_2/(K_1+K_2) \quad (10a)$$

Then,

$$Q_1 = K_1 Q_w/(K_1+K_2) = \tau_1 Q_w \quad (10b)$$

$$Q_2 = K_2 Q_w/(K_1+K_2) = \tau_2 Q_w \quad (10c)$$

The storage capacity ratio,

$$\omega = \phi_2 C_2/(\phi_1 C_1 + \phi_2 C_2) \quad (11)$$

The interporosity flow parameter,

$$\lambda = \frac{\alpha K_1 H^2}{K_1 + K_2} \quad (12)$$

Taking dimensionless transforms, Equations (6a) and (6b) are changed to

$$\beta(\frac{\partial^2 P_{D1}}{\partial x_D^2} + \frac{\partial^2 P_{D1}}{\partial y_D^2} + \frac{\partial^2 P_{D1}}{\partial z_D^2}) + \lambda(P_{D2} - P_{D1}) = (1-\omega)\frac{\partial P_{D1}}{\partial t_D} - \tau_1\delta(x_D - x'_D)\delta(y_D)\delta(z_D - z_{wD}) \quad (13a)$$

$$(1-\beta)(\frac{\partial^2 P_{D2}}{\partial x_D^2} + \frac{\partial^2 P_{D2}}{\partial y_D^2} + \frac{\partial^2 P_{D2}}{\partial z_D^2}) - \lambda(P_{D2} - P_{D1}) = \omega\frac{\partial P_{D2}}{\partial t_D} - \tau_2\delta(x_D - x'_D)\delta(y_D)\delta(z_D - z_{wD}) \quad (13b)$$

Taking the Laplace transform and double Fourier transform of Equations (13a) and (13b), using boundary conditions and initial condition, we obtain the point sink solution at (x'_D, 0, Z_w) below:

$$P_{D2}(x'_D, z_{wD}, t_D) = -\sum_{n=0}^{\infty}\cos(n\pi z_D/H_D)\cos(n\pi z_{wD}/H_D) \times[\tau_1 f_{3,n}(\beta,\lambda,\omega,x_D,y_D,x'_D,t_D) + \tau_2 f_{4,n}(\beta,\lambda,\omega,x_D,y_D,x'_D,t_D)] \quad (14)$$

Where,

$$f_{j,n}(\beta,\lambda,\omega,x_D,y_D,x'_D,t_D) = (\frac{1}{2\pi})\int_{-\infty}^{\infty}\int_{-\infty}^{\infty}F_{j,n}(\beta,\lambda,\omega,\gamma,x'_D,t_D,\xi_1,\xi_2)\exp[i(\xi_1 x_D + \xi_2 y_D)]d\xi_1 d\xi_2 \quad (j=3,4) \quad (15)$$

And,

$$F_{3,n}(\beta,\lambda,\omega,x'_D,t_D,\xi_1,\xi_2) = [\exp(-i\xi_1 x'_D)/(2\pi H_D d_n) \times\{[\frac{\lambda}{(-\omega)(1-\omega)}]\times[\frac{(a-b)+b\exp(at_D)-a\exp(bt_D)}{ab(a-b)}]\} \quad (16a)$$

$$F_{4,n}(\beta,\lambda,\omega,x'_D,t_D,\xi_1,\xi_2)=[\exp(-i\xi_1 x'_D)/(2\pi H_D d_n)\times\{[\frac{\beta\gamma^2+\lambda}{(-\omega)(1-\omega)}]\times[\frac{(a-b)+b\exp(at_D)-a\exp(bt_D)}{ab(a-b)}]-(\frac{1}{\omega})\times[\frac{\exp(at_D)-\exp(bt_D)}{(a-b)}]\} \quad (16b)$$

In the above equations,

$$a=(-U+\sqrt{U^2-4V})/2,\quad b=(-U-\sqrt{U^2-4V})/2, \quad (17)$$

$$U=(-2\beta\omega\gamma^2-\gamma^2+\beta\gamma^2-\lambda+\omega\gamma^2)/(-\omega+\omega^2) \quad (18a)$$

$$V=(-\beta\gamma^4+\beta^2\gamma^4-\lambda\gamma^2)/(-\omega+\omega^2) \quad (18b)$$

$$\gamma^2=\xi_1^2+\xi_2^2+(n\pi/H_D)^2 \quad (18c)$$

Uniform line sink solution

Assume the horizontal well is a uniform line sink which is located between point at (0, 0, Z_w) and point at (L, 0, Z_w), the dimensionless line sink is located between point at (0, 0, Z_w) and point at (L_D, 0, Z_{wD}), according to the Principle of Superposition, and recall Equation (4), the dimensionless pressure at the wellbore point at (x_D, 0, Z_{wD}) is

$$P_{wD}(x_D;x'_D,z_{wD},t_D)=-\sum_{n=0}^{\infty}\cos(n\pi z_D/H_D)\cos(n\pi z_{wD}/H_D)\times[\tau_1 g_{3,n}(\beta,\lambda,\omega,x_D,y_D,x'_D,t_D)+\tau_2 g_{4,n}(\beta,\lambda,\omega,x_D,y_D,x'_D,t_D)] \quad (19)$$

Where,

$$g_{j,n}(\beta,\lambda,\omega,x_D,y_D,x'_D,t_D)=\int_0^{L_D} f_{j,n}(\beta,\lambda,\omega,x_D,y_D,x'_D,t_D)dx'_D,(j=3,4) \quad (20)$$

Recall Equation (15), note that if $h>0$, there holds,

$$\int_{-\infty}^{\infty}\int_{-\infty}^{\infty}F(\xi_1,\xi_2)d\xi_1 d\xi_2=\sum_{l=-\infty}^{\infty}\sum_{m=-\infty}^{\infty}\int_{lh}^{(l+1)h}\int_{mh}^{(m+1)h}F(\xi_1,\xi_2)d\xi_1 d\xi_2 \quad (21)$$

Using Mean Value Theorem there holds

$$f_{j,n}(x_D,y_D)\approx(\frac{1}{2\pi})\sum_{l=-20}^{20}\sum_{m=-20}^{20}h^2 F_{j,n}[(l+1/2)h,(m+1/2)h],(j=3,4) \quad (22)$$

Combining Equations (19), (20), (21) and (22), the horizontal wellbore pressure can be obtained.

At very early time,

$$P_{wD}=(\frac{2\chi}{L_D\sqrt{\pi}})\sqrt{t_D}-(\frac{\chi^2}{2L_D^2})t_D \quad (23)$$

Where

$$\chi=\frac{1+D}{D\sqrt{\eta_1}+\sqrt{\eta_2}} \quad (24a)$$

And

$$\eta_1=(1-\omega)/\beta,\eta_2=\omega(1+D) \quad (24b)$$

When $t_D<0.05, L_D>5$, Equation (23) reduces to

$$P_{wD}=(\frac{2\chi}{L_D\sqrt{\pi}})\sqrt{t_D} \quad (25)$$

At very late time, if $D<0.25, t_D>10^3$, there holds

$$P_{wD}=\frac{1}{2}\{1.423+\ln(t_D)+Ei[\frac{-\lambda t_D}{\omega(1-\omega)}]-Ei(\frac{-\lambda t_D}{1-\omega})\}-(\frac{1}{4})\ln[4\sin(\pi z_{wD})\sin(\pi R_{wD})] \quad (26a)$$

When $t_D>10^4$, Equation (26a) reduces to

$$P_{wD}=\frac{1}{2}[1.423+\ln(t_D)]-(\frac{1}{4})\ln[4\sin(\pi z_{wD})\sin(\pi R_{wD})] \quad (26b)$$

2.1. Flow regimes

A number of different flow regimes can be found while analyzing transient-pressure responses in horizontal wells. One or more of these flow regimes could be missing or masked depending on the reservoir parameters.

As production starts, the pressure transient will move perpendicular to the wellbore, then radial flow is formed. This flow regime has been recognized as early time radial flow and its duration is very short when in thin reservoirs or high vertical permeability reservoirs.

Typically, there is a substantial storage volume associated with a horizontal wellbore which can have serious consequences on the effectiveness of a pressure transient test, even when the measurement tool is located below a downhole shut-in device. Kuchuk et al. (1990) noted that the storage effect in a horizontal well typically lasts longer than that for a vertical well in the same formation, because of (a) greater wellbore volume; (b) anisotropy reduces the effective permeability for a horizontal well. Daviau et al. (1985) showed that the first semilog straight line associated with early time radial flow almost always disappears because of the effects of wellbore storage. Thus, early time radial flow regime is not studied in this paper.

Often, the length of the horizontal well is much greater than the reservoir thickness, which contributes to the formation of the second primary flow regime. This is known as intermediate time linear flow regime and is

developed when pressure disturbance reaches both the upper and lower boundaries of the reservoir.

In the absence of a constant-pressure source and no boundaries to horizontal flow over a reasonable distance, flow towards the horizontal wellbore becomes effectively radial in nature after a long enough time, with the horizontal plane acting somewhat like a point source, this flow regime, called late time radial flow regime. Between intermediate time linear flow regime and late time radial flow regime, there exists a transition period. As shown in Figure-2, the reservoir has infinite lateral extension, there does not exist late time linear flow regime, pseudo-steady state cannot be reached and is not studied in this paper.

2.2. Dual-porosity, dual-permeability behavior

When dual-porosity, dual-permeability responses are plotted with the dimensionless pressure P_D versus the dimensionless time t_D, the curves are defined with D, ω, and λ. D and ω define the contrast between matrix block system and fracture system, λ defines the interaction between the two systems. Because pressure behavior is slightly affected by the vertical coordinate of center of the horizontal well, so we always assume $z_w = H/2$, and the length of the horizontal well is much greater than the reservoir thickness, there holds $L/H > 5$. And we assume skin factor S=0 in the following discussions.

Figures-4 and 5 show the influence of permeability ratio D on bottomhole pressure drop. With increasing permeability ratio, the characteristic trough of pressure derivative on the log-log plot will become shallow, the intermediate segment of the semilog plot of pressure versus time will shorten. The intermediate segment almost vanishes with unity permeability ratio (D=1).

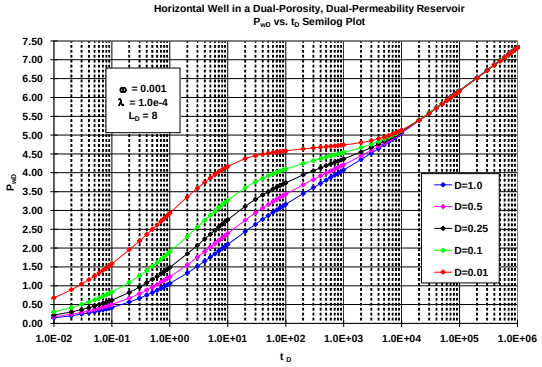

Figure-4. Semi-Log plot of influence of permeability ratio D on $P_{wD.}$

On log-log derivative plot, straight lines with one half slope can be found for each value of D at early time, then intermediate time transition behavior establishes, the smaller D, the deeper the characteristic trough. At late time, the system reaches a homogeneous behavior characterizing the total permeability thickness, total storativity, pressure derivative reaches a constant with a value of 0.5.

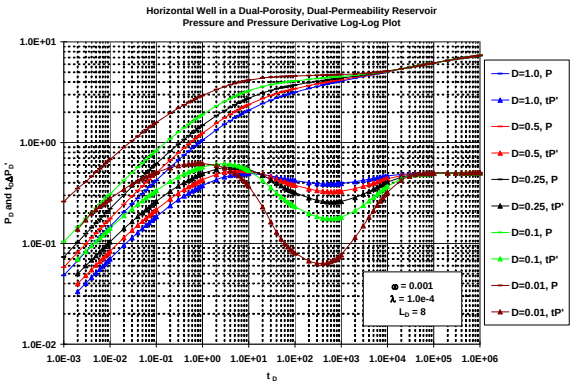

Figure-5. Log-Log plot of influence of permeability ratio D on $P_{wD.}$

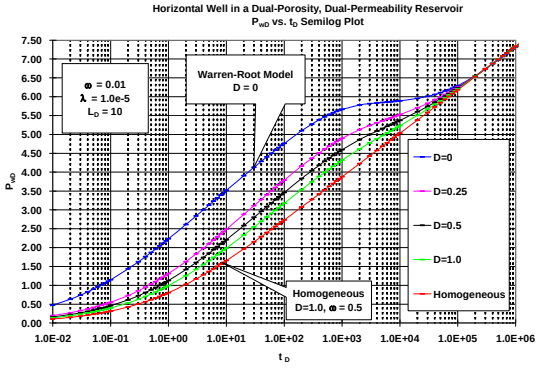

Figure-6. Semi-Log plot of the two extreme cases D=0 and D=1.

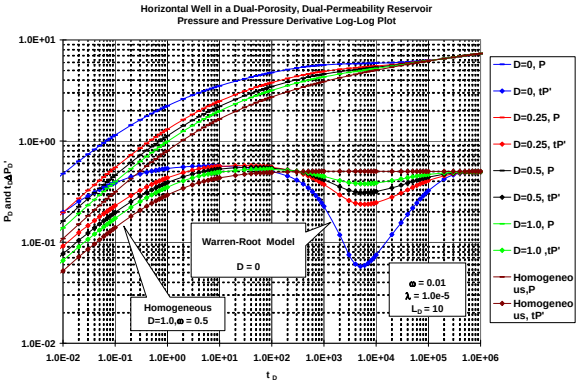

Figure-7. Log-Log plot of the two extreme cases D=0 and D=1.

The results of the well-known Warren and Root's model in which the flow within matrix blocks is neglected (D=0**)** and the results in the case of homogeneous medium

(D=1, ω=0.5) are shown as two special and extreme cases in Figures-6 and 7.

Figures-8, 9 and 10 show the influence of storativity ratio ω and permeability ratio D on bottomhole pressure drops when λ is specified. It can be found that if D and λ are specified, the result of increasing ω is similar to that of increasing D in a semilog plot. When ω increases, the intermediate segment shortens and almost disappears.

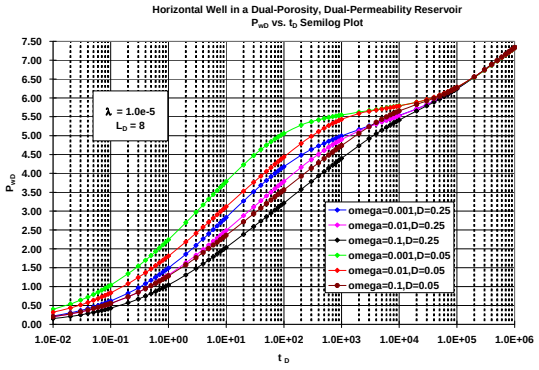

Figure-8. Semi-Log plot of influence of ω and D on P_{wD}.

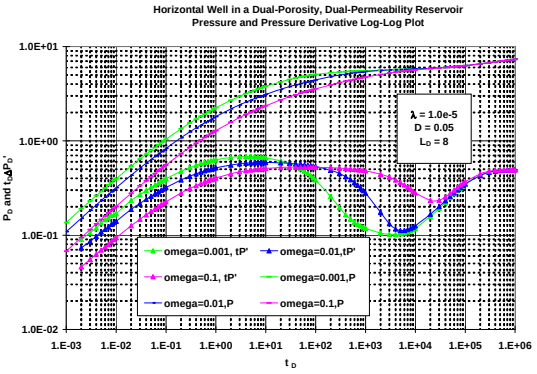

Figure-9. Log-Log plot of influence of ω and D on P_{wD} (D=0.05).

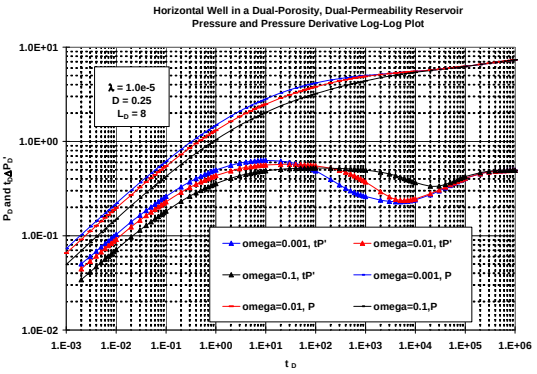

Figure-10. Log-Log plot of influence of ω and D on P_{wD} (D=0.25).

Figures-11, 12 and 13 show the influence of interporosity flow parameter λ and permeability ratio D on bottom hole pressure drop when ω is specified. It can be found that if D and ω are specified, on the log-log plot, different curves corresponding to different values of λ converge to a one-half slope straight line at early time, because at early time, before the interporosity flow is fully established, the response is the same for the reservoirs with different λ. On the semi-log plot, with the increasing λ, the intermediate segment shortens.

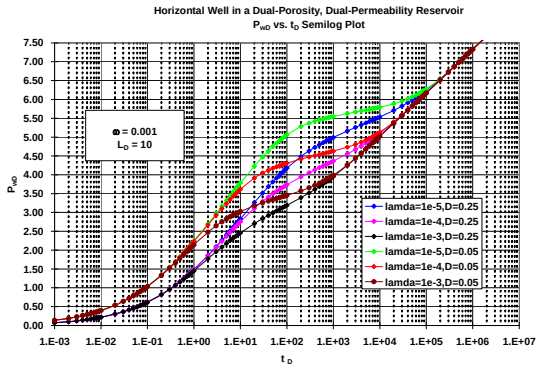

Figure-11. Semi-Log plot of influence of λ and D on P_{wD}.

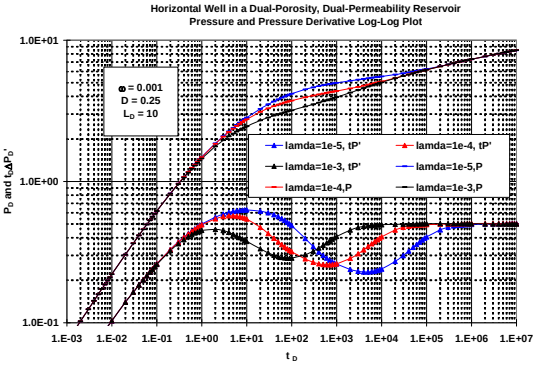

Figure-12. Log-Log plot of influence of λ and D on P_{wD} (D=0.25).

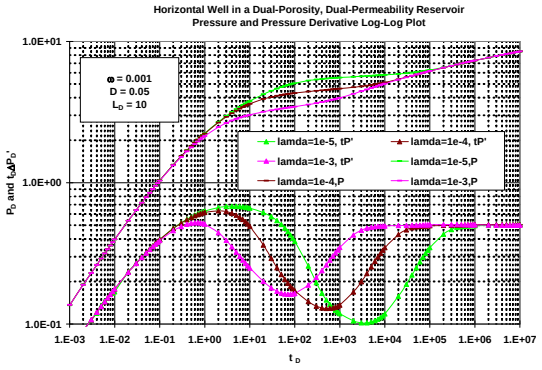

Figure-13. Log-Log plot of influence of λ and D on P_{wD} (D=0.05).

All the characteristic parameters D, ω, and λ of a dual-porosity, dual-permeability medium play their role only in the early and transition stages, and all curves for various D, ω and λ converge to the same straight line segment. The essential nature of fluid flow through a double porosity, single permeability medium revealed by Warren and Root's model that in a semilog plot there appear an intermediate segment, weakens with the increasing of permeability ratio D.

The pressure response exhibits linear flow when pressure transient reaches the upper and lower impermeable boundaries. Before this period can be fully developed, however, the matrix begins to contribute, significantly, to the fracture flow. Subsequently, the transition period becomes dominant and the minimum coordinates are observed. After the transition period, the late time, infinite-acting radial flow period is present; the reservoir reaches a homogeneous behavior characterizing the total producing system.

3. *TDS* TECHNIQUE

Tiab's Direct Synthesis couples the characteristic points and lines of pressure and pressure derivative data with exact analytical solutions, resulting in estimates of reservoir parameters.

The enhanced resolution of the flow regimes from derivative curve results in accurate analysis of the flow regimes which is observed during the well test. The derivative follows the one-half slope straight line at early time, reaches a maximum, the drops below the 0.5 line in a transition, and finally reaches the 0.5 stabilization when radial flow in the equivalent homogeneous total system is reached. During the transition, the shape of the derivative valley is a function of the contrast of storativity and permeability between matrix system and fracture system. The pressure derivative response exhibits the characteristic trough with the associated minimum coordinates.

Empirical expressions are developed to determine the storage capacity ratio ω from the ratio of the minimum to late time radial pressure derivative coordinates:

Table-1. Determine storage capacity ratio ω by the normalized minimum pressure derivative points.

D	λ	a	b	c	d	e
0.01	1.0E-07	-0.078	1.704	-11.085	33.803	-34.383
	1.0E-06	-0.094	1.946	-12.451	36.977	-37.003
	1.0E-05	-0.136	2.562	-15.848	44.846	-43.551
	1.0E-04	-0.232	3.792	-21.729	56.391	-51.294
0.05	1.0E-07	-0.299	3.969	-18.669	39.333	-28.985
	1.0E-06	-0.452	5.774	-26.559	54.244	-39.326
	1.0E-05	-0.822	9.808	-42.914	83.061	-58.021
	1.0E-04	-1.757	18.871	-75.260	132.750	-85.655
0.1	1.0E-07	-0.656	6.703	-25.081	41.601	-24.538
	1.0E-06	-1.154	11.524	-42.451	69.028	-40.595
	1.0E-05	-2.445	23.220	-81.875	127.380	-72.650
	1.0E-04	-5.318	46.333	-150.650	216.560	-115.080
0.25	1.0E-07	-1.567	10.780	-27.342	30.168	-11.595
	1.0E-06	-4.439	31.589	-83.724	97.781	-41.889
	1.0E-05	-13.395	93.282	-242.520	278.680	-118.870
	1.0E-04	-29.848	196.360	-483.210	526.630	-213.920
0.5	1.0E-07	-2.4931	11.599	-18.226	9.7993	0.000
	1.0E-06	-6.769	36.070	-70.849	60.158	-18.103
	1.0E-05	-45.942	258.900	-545.510	508.830	-176.900
	1.0E-04	-127.330	695.190	-1421.000	1288.100	-436.530

$$\omega = a + b\left(\frac{(t*\Delta P')_{\min}}{(t*\Delta P')_r}\right) + c\left(\frac{(t*\Delta P')_{\min}}{(t*\Delta P')_r}\right)^2 + d\left(\frac{(t*\Delta P')_{\min}}{(t*\Delta P')_r}\right)^3 + e\left(\frac{(t*\Delta P')_{\min}}{(t*\Delta P')_r}\right)^4 \quad (27)$$

where the subscripts r denotes the late time radial flow period. Table-1 lists the coefficients a, b, c, d and e used in Equation (27) for different D and λ, which are valid from $0 < \omega < 0.1$.

The ratio of the minimum to late time radial pressure derivative coordinates develops a correlation which can immediately determine the interporosity parameter λ by the following equation:

$$\log(1/\lambda) = a + b\left(\frac{(t*\Delta P')_{\min}}{(t*\Delta P')_r}\right) + c\left(\frac{(t*\Delta P')_{\min}}{(t*\Delta P')_r}\right)^2 + d\left(\frac{(t*\Delta P')_{\min}}{(t*\Delta P')_r}\right)^3 \quad (28)$$

Table-2 lists the coefficients a, b, c and d used in Equation (28) for different D and ω, which are valid from. $10^{-8} \le \lambda \le 10^{-3}$.

We introduce the following notations:

$$K_t = K_1 + K_2 \quad (29a)$$

$$(\phi C)_t = \phi_1 C_1 + \phi_2 C_2 \quad (2bb)$$

In oil field units, and only include mechanical skin factor, Equation (25) is expressed as

Table-2. Determine interporosity parameter λ by the normalized minimum pressure derivative points.

D	ω	a	b	c	d
0.01	0.001	14.7	-215.7	1528.9	-3850.4
	0.01	57.7	-1060.8	7014.6	-15512.0
	0.05	2189.1	-22453.0	76959.0	-87984.0
	0.1	6521.8	-49899.0	127432.0	-108560.0
0.05	0.001	24.1	-200.4	698.2	-867.4
	0.01	56.4	-545.5	1926.8	-2313.8
	0.05	459.2	-3283.8	7948.2	-6462.9
	0.1	2269.8	-13754.0	27893.0	-18900.0
0.1	0.001	37.2	-252.9	670.4	-624.7
	0.01	74.3	-547.1	1447.8	-1306.2
	0.05	422.3	-2500.5	5026.9	-3402.8
	0.1	2254.0	-11853.0	20871.0	-12284.0
0.25	0.001	81.1	-420.9	793.1	-517.2
	0.01	155.6	-834.8	1559.0	-988.4
	0.05	754.7	-3543.6	5620.2	-2996.0
	0.1	5366.1	-23304.0	33820.0	-16390.0
0.5	0.001	207.9	-921.8	1420.6	-746.1
	0.01	421.7	-1878.3	2846.9	-1454.1
	0.05	2596.6	-10536.0	14324.0	-6514.1
	0.1	16804.0	-63199.0	79315.0	-33207.0

$$P_{ini}-P_w=(\frac{2.588\chi BQ_w}{LH})(\frac{\mu t}{K_t(\phi C)_t})^{1/2}+(\frac{141.2\mu BQ_w}{K_tH})S_m \quad (30)$$

On theΔP_w vs. $t^{1/2}$ plot, we can obtain a straight line with a slope below:

$$m_l=(\frac{2.588\chi BQ_w}{LH})(\frac{\mu}{K_t(\phi C)_t})^{1/2} \quad (31)$$

Then,

$$\chi=(\frac{LHm_l}{2.588BQ_w})(\frac{K_t(\phi C)_t}{\mu})^{1/2} \quad (32a)$$

$$K_t=(\frac{\mu}{(\phi C)_t})(\frac{2.588\chi BQ_w}{LHm_l})^2 \quad (32b)$$

And skin factor can be calculated by

$$S_m=(\frac{0.01833\chi}{L})(\frac{K_t}{\mu(\phi C)_t})^{1/2}(\frac{P_{ini}-P_w|_{t=0}}{m_l}) \quad (33)$$

Where $P_w|_{t=0}$ is the pressure at t=0, obtained by extrapolating the straight line section back to this time. For the pressure derivative, there holds

$$(t*\Delta P')_l=\left(\frac{m_l}{2}\right)t^{1/2} \quad (34a)$$

For t=1 hour,

$$(t*\Delta P')_{l1}=\frac{m_l}{2} \quad (34b)$$

Then,

$$K_t=(\frac{\mu}{(\varphi C)_t})(\frac{1.294\chi BQ_w}{LH(t*\Delta P')_{l1}})^2 \quad (35)$$

And

$$S_m=(\frac{0.00916\chi}{L})(\frac{K_tt_l}{\mu(\phi C)_t})^{1/2}(\frac{\Delta P_l}{(t\Delta P')_l}-2.0) \quad (36)$$

In oil field units, and only consider mechanical skin factor, Equation (26b) is expressed as

$$P_{ini}-P_w=(\frac{70.6\mu BQ_w}{K_tH})\{1.423+\ln(\frac{K_tt}{\mu(\phi C)_tH^2})-(\frac{H}{L})\ln[4\sin(\frac{\pi z_w}{H})\sin(\frac{\pi R_w}{H})]+(\frac{H}{2L})S_m\} \quad (37a)$$

If we use common log, then

$$P_{ini}-P_w=(\frac{162.6\mu BQ_w}{K_tH})\{0.618+\log(\frac{K_tt}{\mu(\phi C)_tH^2})-(\frac{H}{L})\log[4\sin(\frac{\pi z_w}{H})\sin(\frac{\pi R_w}{H})]+0.217(\frac{H}{L})S_m\} \quad (37b)$$

On the semilog plot, we can obtain a straight line with a slope below:

$$m_r=\frac{162.6\mu BQ_w}{K_tH} \quad (38)$$

So

$$K_t=\frac{162.6\mu BQ_w}{m_rH} \quad (39)$$

Skin factor can be calculated by

$$S_m=4.608(\frac{L}{H})\{(\frac{P_{ini}-P_w|_{1hr}}{m_r})-0.618-\log(\frac{K_t}{\mu(\phi C)_tH^2})+(\frac{H}{L})\log[4\sin(\frac{\pi z_w}{H})\sin(\frac{\pi R_w}{H})]\} \quad (40)$$

From Equation (37a), we obtain

$$(t*\Delta P')_r=\frac{70.6\mu BQ_w}{K_tH} \quad (41)$$

Then

$$K_t = \frac{70.6\mu BQ_w}{(t\Delta P')_r H} \quad (42)$$

And skin factor can be calculated by

$$S_m = (\frac{2L}{H})\{\frac{\Delta P_r}{(t*\Delta P')_r} - 1.423 - \ln(\frac{K_t t_r}{\mu(\varphi C)_t H^2}) + (\frac{H}{L})\ln[4\sin(\frac{\pi z_w}{H})\sin(\frac{\pi R_w}{H})]\} \quad (43)$$

Step by step procedure

Case one:

All intermediate time linear flow, transition flow and late time radial flow regimes are observed.

Step-1: Identify the late time radial flow period represented by a constant derivative line and calculate the total permeability K_t from Equation (42), if $_D$ is given, solve Equations (7a) and (29a), then obtain K_1 and K_2.

Step-2: Calculate χ from Equation (32a), if ω is given, then solve Equation (24a) to estimate D. If D is given, Substitute Equation (24b) into Equation (24a), also solve Equation (24a) to estimate ω.

Step-3: Identify the intermediate time linear flow period represented by one-half slope derivative line, for verification purpose; calculate the total permeability K_t again from Equation (35).

Step-4: Identify the minimum pressure derivative coordinate and normalize with respect to the late time radial pressure derivative line. Substituting this ratio into Equation (28) results in an estimate for λ, and calculate ω by Equation (27), however, these methods are less reliable and require more information to estimate λ and ω.

Step-5: Select convenient points within well-defined horizontal well flow regimes on the pressure and pressure derivative curves. Substitute these points into Equations (33), (36), (40), (43) and solve for mechanical skin factor.

Case two:

Late time radial flow period is not observed.

Step-1: Calculate χ from Equation (24a), assuming ω and D are given.

Step-2: Identify the intermediate time linear flow period represented by one-half slope derivative line; calculate the total permeability K_t from Eq. (32b). Solve Equations (7a) and (29a), then obtain K_1 and K_2.

Step-3: Select a convenient point during intermediate time linear flow regime on the pressure and pressure derivative curves. Substitute this point into Equations (33) and (36), and solve for mechanical skin factor.

Case three

Intermediate time linear flow period is not observed.

Step-1: Identify the late time radial flow period represented by a constant derivative line and calculate the total permeability K_t from Eq. (42), or from the slope of the straight line on the semi-log plot, calculate K_t from Equation (39). If D is given, solve Equations (7a) and (29a), then obtain K_1 and K_2.

Step-2: Locate the minimum derivative point (assuming it is present), and normalize with respect to the late time radial pressure derivative line, then determine ω and λ by Equations (27) and (28), respectively.

Step-3: Select a convenient point during late time radial flow regime on the pressure and pressure derivative curves. Substitute this point into Equations (40) and (43), and solve for mechanical skin factor.

4. EXAMPLES

4.1. Example one

Only early time pressure drop data are available. Reservoir and well data are in Table-3, pressure drop data are in Table-4.

Solution: This problem matches Case Two.

Step-1: From ΔP_w vs. $t^{0.5}$ plot (see Figure-14), we obtain

$$m_l = 66.52(psia/hr^{1/2})$$

$$\Delta P_w|_{t=0} = 20(psia)$$

Since D = 0.1 and ω = 0.05, use Equations (24a) and (24b), we obtain

$$\chi = 1.8826$$

Step-2: Use Equation (32b), we have

$$K_t = (\frac{1.147}{0.11(1.35\times10^{-5})}) \times (\frac{2.588(1.8826)(1.357)(2500)}{(500)(40)(66.52)})^2 = 119.2(mD)$$

Then solve Equations (7a) and (29a), and obtain

$$K_1 = 10.8(mD) \qquad K_2 = 108.4(mD)$$

Step-3: From Figure 14, we obtain

$$\Delta P_w|_{t=0} = 20(psia)$$

From Equation (33), we have

$$S_m = \left(\frac{0.01833(1.8826)}{500}\right) \times \left(\frac{119.2}{1.147(0.11)(1.35\times10^{-5})}\right)^{1/2}\left(\frac{20}{66.52}\right) = 0.17$$

From log-log plot (see Figure-15), we obtain a one-half slope straight line, we choose

Table-3. Reservoir and well data for example one.

Parameter	Data	Parameter	Data
ϕ_t	0.11	λ	1.00E-04
$C_t(psia^{-1})$	1.35E-05	ω	0.05
H (ft)	40	Q (STB/D)	2500
L (ft)	500	B (RB/STB)	1.357
μ (cp)	1.147	D	0.1
R_w (ft)	0.5	P_{ini} (psia)	3860

Table-4. Pressure data for example one.

t (hr)	P_w (psia)	t (hr)	P_w (psia)
0.0015	3836.71	0.0760	3820.58
0.0030	3835.67	0.0950	3818.24
0.0060	3834.19	0.1200	3815.44
0.0090	3833.05	0.1500	3812.40
0.0120	3832.07	0.1900	3808.72
0.0150	3831.21	0.2400	3804.54
0.0190	3830.17	0.3000	3799.97
0.0240	3829.02	0.3800	3794.41
0.0310	3827.57	0.4700	3788.68
0.0380	3826.27	0.6000	3781.07
0.0470	3824.75	0.7800	3771.48
0.0610	3822.63	0.9600	3762.64

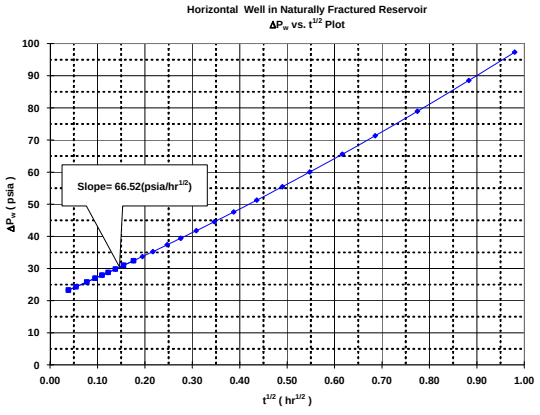

Figure-14. ΔP_w vs. $t^{1/2}$ plot for example one.

$$\Delta P_l = 26.9(psia), (t*\Delta P')_l = 3.16(psia)$$

Use Equation (36), then

$$S_m = \left(\frac{0.00916(1.8826)}{500}\right) \times \left(\frac{119.2}{1.147(0.11)(1.35\times10^{-5})}\right)^{1/2}\left(\frac{26.9}{3.16}-2\right) = 0.18$$

Only intermediate time and late time pressure drop data are available. Reservoir and well data are the same as shown in Table-3, pressure drop data are in Table-5.

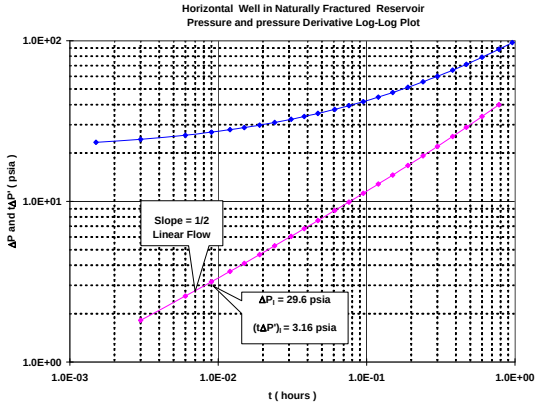

Figure-15. Log-Log plot for example one.

4.2. Example Two

Table-5. Pressure data for example two.

t (hr)	P_w (psia)	t (hr)	P_w (psia)
9.6	3399.20	93.0	3356.25
12.3	3395.12	105.0	3351.92
15.0	3392.43	129.0	3343.88
18.0	3390.09	141.0	3340.14
21.0	3388.14	150.0	3337.44
24.0	3386.40	168.0	3332.32
27.0	3384.77	194.0	3325.49
30.0	3383.22	220.0	3319.25
33.0	3381.72	264.0	3309.83
39.0	3378.83	295.0	3303.91
45.0	3376.03	321.0	3299.34
51.0	3373.31	352.0	3294.29
57.0	3370.68	393.0	3288.18
63.0	3368.11	437.0	3282.26
69.0	3365.61	470.0	3278.17
81.0	3360.81	500.0	3274.68

Solution: This problem matches case three.

Step-1: From semilog plot see Figure-16), we obtain

$$m_r = 130(psia/cycle)$$

$$\Delta P_w|_{t=1hr} = 275(psia)$$

From Equation (39),

$$K_t = \frac{162.6(1.147)(2500)(1.357)}{(130)(40)} = 121.5(mD)$$

Then solve Equations (7a) and (29a), and obtain

$$K_1 = 11.0(mD) \qquad K_2 = 110.5(mD)$$

From log-log plot (see Figure-17),

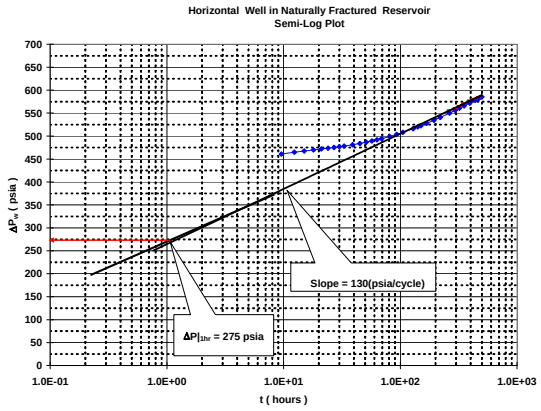

Figure-16. ΔP_w vs. semilog t plot for example two.

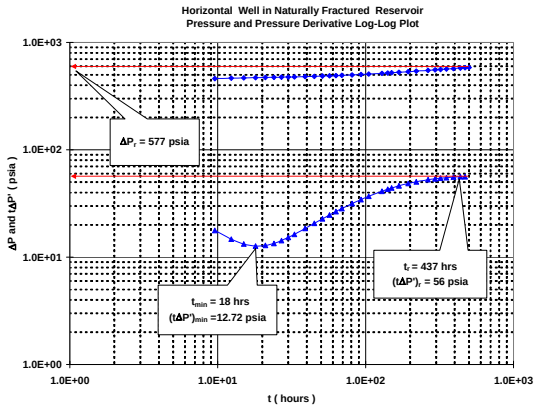

Figure-17. Log-Log plot for example two.

$$t_r = 437(hrs), (t*\Delta P')_r = 56(psia)$$

From Equation (42), we have

$$K_t = \frac{70.6(1.147)(2500)(1.357)}{(56)(40)} = 122.1(mD)$$

Step-2: The minimum derivative point is

$$t_{\min} = 18.0(hrs), \quad (t*\Delta P')_{\min} = 12.72(psia)$$

and

$$(t*\Delta P')_r = 56(psia)$$

We may use Equations (27) and (28) to obtain roughly estimations of ω and λ.

$$\omega = 0.1, \qquad \lambda = 8\times10^{-4}$$

The above results indicate that Equations (27) and (28) and the parameters in Table-1 and Table-2 are less reliable.

Step-3: From Figure 16,

$$m_r = 130(psia/cycle), \quad \Delta P_w|_{t=1hr} = 275(psia)$$

Use Equation (40), we obtain

$$S_m = 0.21$$

From Figure 17,

$$t_r = 437(hrs), \quad (t*\Delta P')_r = 56(psia), \quad \Delta P_r = 577(psia)$$

Use Equation (43), then

$$S_m = 0.21$$

We may use the value of K_t obtained in Example Two to verify χ and D. Use Equation (32a),

$$\chi = \left(\frac{(500)(40)(66.52)}{2.588(1.357)(2500)}\right) \times \left(\frac{121.5(0.11)(1.35\times10^{-5})}{1.147}\right)^{1/2} = 1.9$$

Then use Equation (24a), we have

$$1.9 = \frac{1+D}{D\sqrt{(1-0.05)(1+D)/D} + \sqrt{0.05(1+D)}}$$

Solve for D,

$$D = 0.11$$

CONCLUSIONS

a) This paper presents an alternative analytical solution to the system of pressure equations of horizontal wells in a dual-porosity, dual-permeability naturally fractured reservoir.

b) The flow within matrix blocks will weaken the essential nature of fluid flow through a dual-porosity, single permeability medium revealed by Warren-Root

model. With increasing permeability ratio D, the characteristic trough of pressure derivative on the log-log plot will become shallow; the intermediate segment of the semilog plot of pressure versus time will shorten. The intermediate segment almost vanishes with unity permeability ratio. The result of increasing ω is similar to that of increasing D in a semi-log plot.

c) The pressure response exhibits linear flow when pressure transient reaches the upper and lower impermeable boundaries, subsequently, the transition period becomes dominant and the minimum coordinates are observed. After the transition period, the late time, infinite-acting radial flow period is present; the reservoir reaches a homogeneous behavior characterizing the total producing system.

d) For intermediate time linear flow and late time radial flow, the simplified pressure drop equations are presented, which can be used to calculate total permeability and mechanical skin factor.

ACKNOWLEDGMENTS

This paper was presented at the 2009 SPE Middle East Oil and Gas Show and Conference held in the Bahrain International Exhibition Centre, Kingdom of Bahrain, 15-18 March, 2009 (SPE120103). The authors would like to thank Society of Petroleum Engineers and The Petroleum Institute at Abu Dhabi, United Arab Emirates, for permission to publish this paper.

REFERENCES

Aguilera R. and Ng M. C. 1991. Transient pressure analysis of horizontal wells in anisotropic naturally fractured reservoirs. SPEFE. 95-100.

Barenblatt G.I., Zheltov Y. P. and Kochina I.N. 1960. Basic concepts in the theory of seepage of homogeneous liquids in fissured rocks. Prik. Matem. Mekh. 24(5): 852-864. (in Russian).

Chen Z.X. and Jiang L.S. 1980. Exact solution for the system of flow equations through a medium with double-porosity, Scientia Sinica. 28(7): 880-896. (in Chinese)

Daviau F., Mouronval G., Bourdarot G. and Curutchet P. 1985. Pressure analysis for horizontal wells. Paper SPE 14251 presented at the SPE Annual Technical Conference and Exhibition, Las Vegas, NV.

Engler T. W. and Tiab D. 1996. Analysis of pressure and pressure derivative without type curve matching, 4. Naturally fractured reservoirs. Journal of Petroleum Science and Engineering. 15: 127-138.

Engler T. W. and Tiab D. 1996. Analysis of pressure and pressure derivatives without type-curve matching, 5. Horizontal well tests in naturally fractured reservoirs. Journal of Petroleum Science and Engineering. 15: 139-151.

Engler T. W. and Tiab D. 1996. Analysis of pressure and pressure derivatives without type-curve matching, 6. Horizontal well tests in anisotropic reservoirs. Journal of Petroleum Science and Engineering. 15: 153-168.

Kuchuk F. J., Goode P. A., Brice B. W., Sherard D. W. and Thambynayagam R. K. M. 1990. Pressure transient analysis for horizontal wells. Journal of Petroleum Technology. 974-1031.

Rosa A.J. and Carvalho R.S. 1988. Transient pressure behavior for horizontal wells in naturally fractured reservoirs. Paper SPE 18302 presented at the SPE Annual Technical Conference and Exhibition, Houston, TX.

Tiab D. 1989. Direct type-curve synthesis of pressure transient tests. Paper SPE 18992 presented at the SPE Rocky Moutain Region/Low Permeability Reservoir Symposium, Denver, CO.

Tiab D. 1994. Analysis of pressure and pressure derivatives without type-curve matching: Vertically fractured wells in closed systems. Journal of Petroleum Science and Engineering. 11: 323-333.

Tiab D. 1995. Analysis of pressure and pressure derivatives without type-curve matching - skin and wellbore Storage. Journal of Petroleum Science and Engineering. 12: 171-181.

Warren J.E. and Root P.J. 1963. The behavior of naturally fractured reservoirs. SPE Journal. 245-255.

Nomenclature

D ratio of matrix permeability to fracture permeability
B oil volumetric factor, rb/STB
C compressibility, 1/psi
H formation thickness, ft
K_1 matrix permeability, mD
K_2 fracture permeability, mD
L horizontal well length, ft.
P pressure, psi
Q_w total well flow rate, STB
r radial distance, ft
R_w wellbore radius, ft
S_m mechanical skin factor
t test time, hr
z_w vertical coordinate of center of horizontal well

Greek symbols

α characteristic factor of NFR, $1/ft^2$
β a parameter defined by Eq.(7b)
γ a parameter defined by Eq.(18c)
η_1 a parameter defined by Eq.(24b)
η_2 a parameter defined by Eq.(24b)

Ω drainage domain defined by Eq.(1)
χ a parameter defined by Eq.(24a)
Δ change, drop
ϕ porosity, fraction
μ viscosity, cp
λ interporosity flow parameter, dimensionless
ω storage coefficient, dimensionless
τ_1 a parameter defined by Eq.(9)
τ_2 a parameter defined by Eq.(9)

Subscripts
D dimensionless
ini initial
l intermediate time linear flow period
min minimum
r late time radial flow period
t total
w well
x,*y*,*z* coordinate indicators
1 matrix bulk property
2 fracture bulk property

SI metric conversion factors

$bbl \times 1.589873 \quad E-01 = m^3$
$cp \times 1.0^* \quad E-03 = Pa.s$
$ft \times 3.048^* \quad E-01 = m$
$psi \times 6.894757 \quad E+03 = Pa$
$mD \times 9.86923 \quad E-16 = m^2$

*Conversion factor is exact.

Appendix: Definition of dimensionless variables

$$x_D = x/H, y_D = y/H, z_D = z/H \quad \text{(A-1)}$$

$$H_D = 1, L_D = L/H, z_{wD} = z_w/H \quad \text{(A-2)}$$

$$r_D = r/H, R_{wD} = R_w/H \quad \text{(A-3)}$$

$$P_{Dj} = 2\pi(K_1 + K_2)H(P_{ini} - P_j)/(\mu B Q_w) \quad \text{(j=1, 2) (A-4)}$$

$$t_D = (K_1 + K_2)t/[\mu H^2(\phi_1 C_1 + \phi_2 C_2)] \quad \text{(A-5)}$$